The influence of CO_2 and H_2O on the storage properties of Pt-Ba/Al_2O_3 LNT catalyst studied by FT-IR spectroscopy and transient microreactor experiments

S. Morandi [a], F. Prinetto [a], G. Ghiotti [a], L. Castoldi [b], L. Lietti [b,*], P. Forzatti [b], M. Daturi [c], V. Blasin-Aubé [c]

[a] *Dipartimento di Chimica and NIS, Center of Excellence, Università di Torino, Via P. Giuria 7, 10125 Torino, Italy*
[b] *Laboratory of Catalysis and Catalytic Processes, NEMAS, Center of Excellence, Dipartimento di Energia, Politecnico di Milano, Piazza Leonardo da Vinci 32, 20133 Milano, Italy*
[c] *Laboratoire Catalyse et Spectrochimie, ENSICAEN, Université de Caen, CNRS, 6 Bd Maréchal Juin, F-14050 Caen, France*

Received 7 October 2013
Received in revised form
17 December 2013
Accepted 19 December 2013
Available online 1 February 2014

1. Introduction

"Lean NO_x Traps" (LNTs) represent a viable technology for the reduction of NO_x under lean conditions [1]. These catalytic systems are made by noble metals (e.g. Pt and/or Rh) and NO_x storage elements (Ba and K), supported over a high surface area carrier. The NO_x removal occurs under cyclic conditions by alternating long phases under lean conditions where NO_x are stored on the catalyst surface, with short rich phases during which the stored NO_x are reduced to N_2 by a reductant.

Both the NO_x storage and reduction steps have been extensively investigated by several authors [1–8]. Concerning the storage phase, in previous works of our groups we have used in situ and operando FT-IR spectroscopy and transient flow reactor experiments to gain complementary information on the gas phase composition and the surface species formed during the adsorption of NO_x from NO/O_2 mixture on a model Pt-Ba/Al_2O_3 catalyst [9–11]. In particular the existence of two different pathways has been envisaged for the storage of NO_x:

(i) the first route, hereafter denoted as "nitrate route", implies the preliminary oxidation of NO to NO_2 on Pt sites (reaction (1)), followed by NO_2 storage onto storage compounds in the form of nitrates through a disproportion reaction (reactions (2)+(3)):

$$NO + \frac{1}{2}O_2 \rightarrow NO_2 \quad (1)$$

$$2NO_2 + O^{2-} \rightarrow NO_2^- + NO_3^- \quad (2)$$

$$NO_2^- + NO_2 \rightarrow NO_3^- + NO \quad (3)$$

According to this pathway, nitrites and nitrates are expected at the beginning of the storage (reaction (2)). However in previous studies on NO_2 adsorption [9,10], nitrites are not detected on the surface even at the very beginning of the storage, likely due to their very fast oxidation to nitrate species (reaction (3));

(ii) the second route, hereafter denoted as "nitrite route", is based on the oxidative adsorption of NO at Pt-BaO border leading to

* Corresponding author. Tel.: +39 02 23993272; fax: +39 02 70638173.
E-mail address: luca.lietti@polimi.it (L. Lietti).

the formation of nitrite adspecies according to the stoichiometry of the following overall reaction (4):

$$2NO + \frac{1}{2}O_2 + O^{2-} \rightarrow 2NO_2^- \quad (4)$$

In this case a cooperative effect operates between the noble metal and the nearby storage component so that NO is oxidized and adsorbed as NO_2^- at the Ba site before it is oxidized to NO_2. Notably, at variance to the *nitrate* pathway, the *nitrite* route accomplishes the storage of NO_x in the form of nitrites only. The stored nitrites might be further oxidized to nitrates by O_2, so that the formation of nitrates is expected as consecutive reaction (reaction (5)):

$$NO_2^- + \frac{1}{2}O_2 \rightarrow NO_3^- \quad (5)$$

As shown in [11], the nitrite route is the unique pathway involved in the storage of NO_x at low temperatures (e.g. at 150 °C) from NO/O_2 since relevant amounts of NO_x are stored in the form of nitrites only at such low temperatures and the oxidation of NO to NO_2 is not observed to a significant extent. However at higher temperatures, i.e. above 200–250 °C, the formation of NO_2 and of nitrates is also observed, along with nitrites. Notably, nitrites are the prevalent species at the initial stages of the storage with NO/O_2, while nitrates represent the most abundant adsorbed species after prolonged contact. This suggests that at high temperatures nitrites are intermediates in the formation of nitrates according to reactions (4) + (5). Besides, in the presence of NO_2 the storage of NO_x also occur according to the nitrate pathway.

These conclusions have been reached based on experiments carried out in the absence of CO_2 and H_2O in the gas stream [11], which however are known to affect the NO_x storage behavior of LNT catalysts. Chaugule et al. [12], who investigated the effect of CO_2 on NO_x storage from NO_2/O_2 mixtures at 300 °C on catalysts with different Ba loading, pointed out that nitrates could replace the preformed carbonates and carboxylates in absence of CO_2 in the gas phase. However, in the presence of CO_2 the adsorbed carbonates and carboxylates could not be completely replaced by nitrates even after a long NO_x exposure. Moreover, the amount of pre-adsorbed CO_2 released during NO_x storage correlated well with the amount of NO_x stored on the catalyst with 20 wt.% Ba, but not on the samples with Ba loadings of 8 and 4 wt.%.

Weiss et al. [13] investigated the adsorption of $NO/NO_2/CO_2$ mixtures on BaO/Al_2O_3 and $Pt\text{-}BaO/Al_2O_3$ in the temperature range 150–400 °C. They found that nitrites form rapidly upon exposure of NO/NO_2 mixtures, but the presence of CO_2 limits the NO_x uptake equilibrium due to the unfavorable thermodynamics. This eventually indicates that nitrite formation is an impractical strategy for NO_x removal from CO_2-rich combustion effluent streams. These conclusions have been obtained with NO/NO_2 mixtures and therefore it is also of interest to analyze the effect of CO_2 during NO_x uptake from NO/O_2.

The effect of CO_2 on the NO_x storage from NO_2 and NO/O_2 mixture has also been investigated previously by *in situ* FT-IR spectroscopy and pulse reactor experiments at 350 °C [14]. It has been found that upon adsorption of NO_x from NO/O_2 both in the presence of gas-phase CO_2 and over CO_2 pre-covered $Pt\text{-}Ba/Al_2O_3$ catalyst the NO_x breakthrough is significantly shortened if compared to the CO_2-free experiments. Besides, FT-IR experiments showed a less pronounced nitrite formation. However the NO_x storage capacity of the catalyst after prolonged contact with NO_2 and NO/O_2 mixtures was only slightly affected both in the presence of gas-phase CO_2 and over the CO_2 pre-covered catalysts.

Based on these findings, in order to better clarify the role of CO_2 and H_2O on the NO_x storage and particularly on the formation of nitrite and nitrate adspecies via the *nitrite* and *nitrate* pathways, NO_x adsorption experiments have been carried out starting from NO/O_2 mixtures in the presence and in the absence of CO_2 and/or H_2O over a model $Pt\text{-}Ba/Al_2O_3$ catalyst sample in the temperature range 150–350 °C. *Operando* FTIR spectroscopy and transient flow pulse reactor experiments have been used as complementary techniques to analyze the pathways involved in the storage of NO_x and the effects produced by the presence of CO_2 and H_2O in the feed stream.

2. Experimental

The $Pt\text{-}Ba/Al_2O_3$ (1/20/100, w/w) catalyst sample used in this work was prepared by incipient wetness impregnation of γ-alumina (Versal 250 from UOP) with aqueous solution of dinitro-diamine platinum (Strem Chemicals, 5% Pt in ammonium hydroxide) and then with a solution of barium acetate (Aldrich, 99%). After each impregnation step, the powder was dried overnight in air at 80 °C and calcined at 500 °C for 5 h.

Textural, morphological and structural characterization was already reported in previous works [10,14–16]. Here, we only recall some information of interest. The specific surface area and pore volume measured by N_2 adsorption-desorption at 77 K were 137 m^2/g and 0.81 cm^3/g, respectively. The Pt dispersion, as determined by H_2 chemisorption at 0 °C, was about 70%, in line with the mean Pt particle size measured by HRTEM (1.5 nm) [16]. XRD patterns of the calcined sample showed the presence of micro-crystalline $\gamma\text{-}Al_2O_3$ and crystalline $BaCO_3$ whiterite phase.

The NO_x storage has been investigated in the presence and in the absence of CO_2 and H_2O by transient experiments wherein rectangular step feeds of NO (1000 ppm) have been admitted in $Ar + O_2$ (3%, v/v) flowing into a IR reactor cell (Aabspec CX cell) directly connected to a Thermo Scientific Nicolet 6700 FT-IR spectrometer equipped with a MCT detector for the analysis of the surface species. Experiments have been performed at 150 °C, 200 °C, 250 °C and 350 °C; when CO_2 and H_2O were present in the feed stream their concentration was 1% (v/v) and 2% (v/v), respectively. The cell was loaded with 15 mg of catalyst powder compressed in self-supporting disc (diameter = 13 mm, thickness = 0.1 mm); a total flow of 25 $cm^3\,min^{-1}$ (at 1 atm and 0 °C) has been used. The IR reactor cell was also directly connected to a quadrupole mass spectrometer (Omnistar GSD 301 with a 1 s time-resolution), and a chemiluminescence analyzer (Model 42i-HL MEGATEC) for the analysis of the gas phase.

For the quantitative analysis of the adsorbates, specific calibration experiments were performed combining the FT-IR spectra with the analysis of the output gases by MS, FT-IR (transmission mode) of the gas phase and chemiluminescence, in order to calculate the molar absorption coefficients for each moiety. In particular the same procedure described in [11] has been adopted to evaluate the amount of nitrites (adsorption at 150 °C) and of nitrates (adsorption at 350 °C).

To allow an accurate analysis of the dynamics of the storage phase, dedicated experiments have been performed in a plug-flow microreactor loaded with 60 mg of catalyst powder (70–100 μm) and operating under the same experimental conditions used in FT-IR experiments. A total flow of 100 $cm^3\,min^{-1}$ (at 1 atm and 0 °C) has been used in these experiments, so that the Gas Hourly Space Velocity (GHSV) was exactly the same for both FT-IR and microreactor experiments ($10^5\ cm^3\ g_{cat}^{-1}\ h^{-1}$). The microreactor was directly connected to a mass spectrometer (Balzers QMS 200) and a FT-IR Multigas 2030 (MKS instrument) for the complete analysis of the reaction products.

Before both FTIR and flow-microreactor experiments, the catalyst was conditioned with several lean-rich cycles with NO/O_2 (1000 ppm NO + O_2 3%, v/v) and H_2 (2000 ppm) at 350 °C, with an inert purge in Ar between the lean and rich phase. Several cycles were run until a reproducible behavior was obtained, which cor-

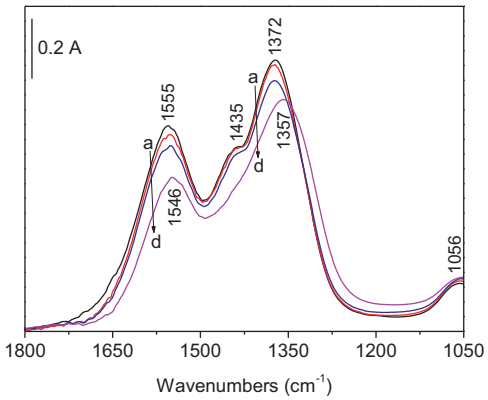

Fig. 1. FT-IR difference spectra of Pt-Ba/Al_2O_3 catalyst upon exposure to a stream of CO_2 (1%, v/v in Ar) at 150 °C (a), 200 °C (b), 250 °C (c) and 350 °C (d). Subtrahend spectrum: catalyst after activation cycles.

responds to the transformation of the Ba carbonate phase into a well-dispersed nanosized BaO phase [16].

Finally, the thermal stability of the surface species involved in the storage in the presence of CO_2, i.e. nitrites, nitrates and carbonates, was investigated by *in situ* FT-IR spectroscopy. For this purpose adsorption of NO/O_2 (1/10 mixture), NO_2 (2 mbar) and CO_2 (2 mbar) was performed at 100 °C to form surface nitrites (the mixture used and the low temperature ensure the formation of only nitrites and not nitrates), nitrates and carbonates, respectively. Then the sample was evacuated at increasing temperature in the range 100–400 °C to investigate the thermal stability of the different species.

To better appreciate the spectral features of surface species, the IR spectra are reported in the figures after subtraction of a spectrum chosen as a background; the subtracting spectrum is always indicated in the figure captions.

3. Results and discussion

3.1. CO_2 adsorption

Before addressing the effect of CO_2 on the NO_x storage, it is important to investigate the surface species formed upon contacting CO_2 in the range 150–350 °C over a conditioned catalyst sample, i.e. subjected to several adsorption-reduction cycles in H_2 in order to remove the carbonates present on the freshly calcined sample. The final step of the conditioning treatment was the reduction by H_2 of the stored NO_x, so that the surface is clean from any adsorbed NO_x species. The results obtained upon contacting the sample with CO_2 at different temperatures are shown in Fig. 1. A relevant point is that the surface species formed upon CO_2 adsorption exhibit spectral features completely different from those of crystalline $BaCO_3$ present on the fresh sample before the conditioning cycles, as already shown by some of us in ref. [14]. At 150 °C, 200 °C and 250 °C absorptions at 1555, 1372 and 1056 cm^{-1}, characteristic of surface bidentate carbonate species adsorbed on the Ba phase (ν(C═O), $\nu_{asym.}$(OCO) and $\nu_{sym.}$(OCO), respectively) [14,17] are present. The shoulder at 1435 cm^{-1} is related to the $\nu_{asym.}(CO_3)$ mode of carbonates, adsorbed on the Ba phase, herein indicated as ionic carbonates and not as monodentate carbonates, as suggested in our previous works [14,16]. This new assignment has been enlightened by dedicated experiments performed on the basis of the results that we obtained about the water effect on nitrates stored onto Pt-Ba/Al_2O_3 catalyst [18]: the dissociative chemisorption of water causes the transformation of bidentate nitrates into highly symmetric species that we call ionic nitrates. As a matter of fact, the effect of water on the adsorbed carbonates is the same observed for nitrates. These experiments have shown that the carbonate band at 1435 cm^{-1} is correlated to another one at 1390 cm^{-1} deriving from the splitting of corresponding double degenerate $\nu_{asym.}(CO_3)$ mode of free carbonates. The very low separation between the two bands suggests the presence of highly symmetric surface species that we call ionic carbonates. Under actual working conditions, the band at 1390 cm^{-1} is covered by the band related to $\nu_{asym.}$(OCO) mode of bidentate carbonate species, mainly present on the surface. Notably, no surface species typical of alumina support, such as organic-like and hydrogen carbonates were observed [19], confirming an extensive spreading of the barium oxide phase, as previously shown [15,16].

At 350 °C (Fig. 1, curve d) the bands related to bidentate carbonates are red-shifted to 1546 and 1357 cm^{-1}. Reasonably, also the band at 1435 cm^{-1} related to ionic carbonates is red-shifted in a way that makes it no more visible due to the superimposition with the band at 1357 cm^{-1} that becomes highly asymmetric. The red-shift of carbonate bands can be related to the decrease of surface coverage and to the spreading of carbonates on the surface due to the temperature increase. The coverage decrease on increasing temperature is evidenced by the intensity loss of the bands.

Similar observations have been reported in a previous paper by Epling et al. [20], who studied the adsorbtion of CO_2 on Pt-Ba/Al_2O_3 NO_x storage-reduction catalyst. Similar features have been described regarding carbonate species except in that organic-like carbon species on alumina have been observed in that case.

Specific experiments have been performed in order to quantify the amount of CO_2 adsorbed over the catalyst surface at different temperature. For this purpose, a flow of CO_2 (1%, v/v) has been admitted to the flow microreactor over a conditioned catalyst at 150 °C, 200 °C, 250 °C and 350 °C until saturation has been achieved. Then the catalyst has been cooled down to RT in inert atmosphere and finally heated up to 500 °C (10 °C/min). Accordingly the amounts of CO_2 stored on the catalyst surface at different temperatures could be evaluated; these amounts range from 2.0×10^{-4} mol/g_{cat} at 350 °C to 4.5×10^{-4} mol/g_{cat} at 150 °C. The largest amount of adsorbed CO_2 corresponds roughly to 30% of the overall Ba loading (considering the formation of $BaCO_3$), and decreases on increasing the temperature, as expected: at 350 °C roughly 13% of the overall Ba loading is involved in carbonate formation. Taking into account that the BaO phase is well dispersed on the surface and that the amount of Ba is close to that of a monolayer, it is reasonable to consider that almost all the Ba sites are exposed at the surface. Accordingly, the large fraction of surface sites not available for carbonate adsorption (greater than 70%) is likely due to steric hindrance and electrostatic repulsion between carbonate species.

3.2. NO_x adsorption in the absence and in the presence of CO_2

In Fig. 2 the FT-IR spectra recorded during the NO_x storage at 150 °C in the different atmospheres are shown. In the absence of CO_2 (Fig. 2A), the storage proceeds with the initial formation of chelating nitrites ($\nu_{sym.}(NO_2)$ and $\nu_{asym.}(NO_2)$ at 1360 and 1210 cm^{-1}, respectively), as already evidenced in our previous work [11]. The surface concentration of these species continues to increase with the NO/O_2 exposure until 20 min (Fig. 2A, curve d). Then a band at 1546 cm^{-1} related to ν(N═O) mode of bidentate nitrates, formed by very slow nitrite oxidation, is also present. These data hence indicate that at 150 °C only the nitrite route is effective in the storage of NO_x.

The analysis of the corresponding gas phase allows the quantification of the total amount of NO_x stored at the end of the adsorption step. This amount is near 3.7×10^{-4} mol/g_{cat}, corresponding to 15%

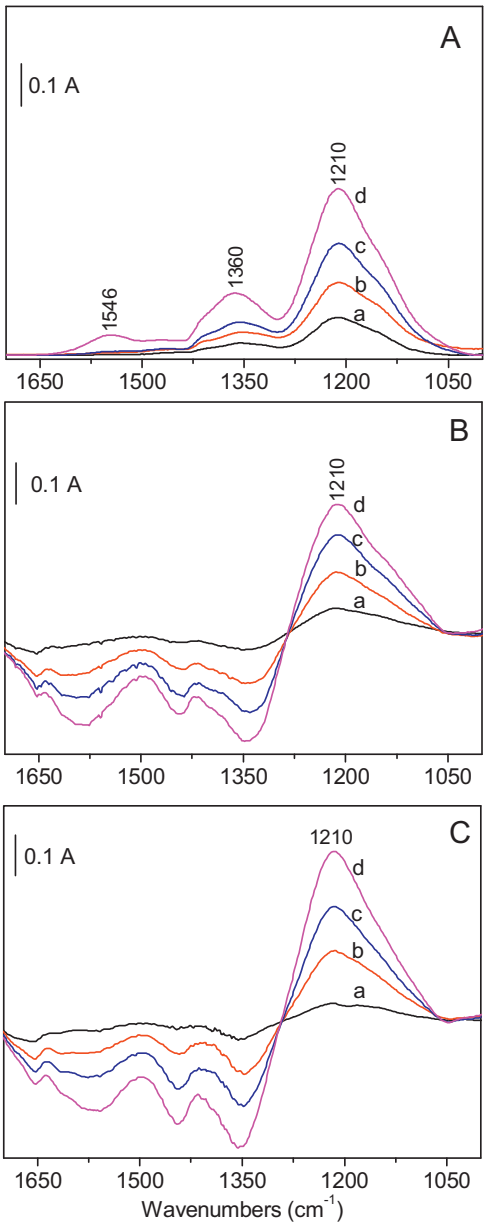

Fig. 2. Section A. FT-IR difference spectra of Pt-Ba/Al_2O_3 catalyst upon exposure to a stream of NO/O_2 (1000 ppm NO in Ar + O_2 3%, v/v) at 150 °C for increasing contact time. FT-IR spectra were recorded after 2 min (a), 5 min (b), 10 min (c) and 20 min (d). Subtrahend spectrum in section A: catalyst after activation cycles. Sections B is the corresponding measurements in the presence of CO_2 (1%, v/v) in the stream. Subtrahend spectrum in section B: catalyst upon exposure to the stream of CO_2 before NO/O_2 admission. Sections C is the corresponding measurements in the presence of CO_2 (1%, v/v) + H_2O (2%, v/v) in the stream. Subtrahend spectrum in section C: catalyst upon exposure to the stream of CO_2 + H_2O before NO/O_2 admission.

of the overall Ba loading by assuming the formation of $Ba(NO_2)_2$ species.

In the presence of CO_2, negative bands appear in the FT-IR spectra (Fig. 2B). In fact the background spectrum is that recorded before NO admission, i.e. under a CO_2/O_2/Ar flow, and accordingly the negative bands are related to the surface carbonate species which are displaced upon NO_x adsorption. Formation of nitrites is observed also in the presence of CO_2; because of the carbonate presence, the evolution of nitrites is observable only through the behavior of the band at 1210 cm^{-1} attributed to the $\nu_{asym.}(NO_2)$ mode. Notably, the increase in intensity of the negative bands related to the displacements of carbonates parallels the increase of the bands of nitrites.

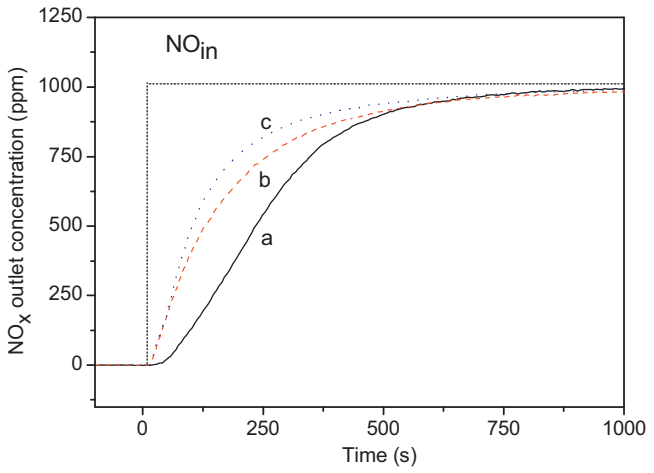

Fig. 3. NO_x outlet concentration during the storage phase at 150 °C over Pt-Ba/Al_2O_3 catalyst; 1000 ppm NO in He + O_2 3%, v/v: curve a in He; curve b + CO_2 (1%, v/v) and curve c + CO_2 (1%, v/v) + H_2O (2%, v/v).

It is also worth to note that the time evolution of the nitrite band is similar to that observed without CO_2 (compare Fig. 2A and B). In this case the gas phase analysis revealed that the total amount of stored NO_x is near 2.4×10^{-4} mol/g_{cat} (10% of the overall Ba loading), i.e. lower than those measured in the absence of CO_2.

Finally in Fig. 2C the results obtained in the presence of both CO_2 and H_2O are reported. The catalytic behavior closely resembles that previously described in the presence of CO_2 only. FT-IR data pointed out that at low temperature (150 °C) nitrites are observed, with amounts that increase with time of stream. The analysis of the region 1700–1280 cm^{-1} also shows the displacement of carbonates during the formation of NO_x, as observed in the case of the presence of CO_2 only. In this case near 3.0×10^{-4} mol/g_{cat} (12% of the overall Ba loading) of NO_x are stored at the end of the storage phase.

As explained in Section 2, to allow an accurate analysis of the dynamics of the storage phase, experiments have been performed in a plug-flow micro-reactor under the same experimental conditions used for the operando FT-IR. The results of the experiments carried out at 150 °C are reported in Fig. 3 in terms of outlet NO_x concentration as a function of time, while the NO_2/NO ratio measured at steady state (i.e. at the end of the NO pulse) is reported in Table 1.

As clearly appears in the Fig. 3, upon NO admission in the absence of CO_2 and H_2O (trace a), a dead time near 30 sec is observed in the NO_x breakthrough. In the presence of CO_2 and of both CO_2 + H_2O the dead time is reduced, i.e. the NO_x breakthrough is observed at the reactor outlet after few seconds. The outlet NO_x concentration increases reaching the inlet value more rapidly in the presence (curve b) than in the absence of CO_2, indicating that the NO_x uptake is slower. Only negligible amounts of NO_2 are observed at the reactor outlet (Table 1), pointing out that the NO oxidation reaction is very slow at this temperature. Note that the presence of water (curve c) in the feed further decreases the NO_2/NO ratio (Table 1), in line with literature data [21–23] showing that water inhibits the oxidation of NO to NO_2.

When CO_2 is present in the feed, the adsorption of NO_x is also accompanied by the evolution of CO_2 (not shown in the Figure) due to the displacement of carbonates by nitrites. This is in line with FT-IR spectra showing the appearance of negative bands. The overall amount of CO_2 exiting the reactor is in line with the occurrence of the following reaction:

$$BaCO_3 + 2NO + \frac{1}{2}O_2 \rightarrow Ba(NO_2)_2 + CO_2 \quad (6)$$

Table 1
Total amount of stored NO_x (mol/g_{cat}), NO_x breakthrough (s) and NO_2/NO ratio at different temperature (150°C, 250°C, 350°C) and different atmospheres (Ar, CO_2, CO_2+H_2O).

	150°C			250°C			350°C		
	Ar	CO_2	$CO_2 + H_2O$	Ar	CO_2	$CO_2 + H_2O$	Ar	CO_2	$CO_2 + H_2O$
Total stored NO_x (10^{-4} mol/g_{cat})	3.7	2.4	3.01	3.6	3.0	2.6	4.3	4.2	4.2
NO_x breakthrough (s)	30	13	13	97	17	17	120	15	15
NO_2/NO ratio	0.022	0.022	0.014	0.35	0.25	0.11	0.56	0.52	0.38

where a 2:1 ratio is expected between the amounts of stored nitrites and desorbed CO_2, close to the measured value.

Experiments have also been performed at 200 °C, 250 °C and 350 °C; for the sake of brevity only experiments performed at 250 °C and 350 °C are illustrated in the following.

Fig. 4 shows FT-IR spectra obtained as a function of time during the NO/O_2 storage at 250 °C in the absence (Fig. 4A), in the presence of CO_2 (Fig. 4B) and in the presence of both CO_2 and water (Fig. 4C). In the absence of CO_2, FT-IR spectra show that mainly nitrites (band at 1210 cm^{-1}) are present after 2 min (Fig. 4A, curve a). After 5 min (Fig. 4A, curve b) nitrites continue to increase and both ionic nitrates ($\nu_{asym.}(NO_3)$ mode split at 1415 and 1326 cm^{-1} and $\nu_{asym.}(NO_3)$ mode at 1035 cm^{-1} [15]) and bidentate nitrates (ν(N=O) mode at 1540 cm^{-1}, the only one visible, start to form. After 20 min (Fig. 4A, curve d), the band at 1210 cm^{-1} related to nitrites decreases in intensity due to the oxidation of nitrites into nitrates and the nitrate bands increase monotonically. Hence these results show that at 250 °C the nitrite pathway is the prevalent route for NO_x storage since nitrates are observed only after nitrite formation. At this temperature nitrates can be formed by nitrite oxidation and by NO_2 dismutation (reactions (2)+(3)). From the gas phase analysis, the total amount of NO_x stored at the end of the storage phase is near 3.6×10^{-4} mol/g_{cat} (14% of the overall Ba loading).

In the presence of CO_2, in the FT-IR spectra (Fig. 4B) the analysis of the region 1700–1280 cm^{-1} is complicated by the presence of negative bands related to displaced carbonates, as observed at 150 °C, but now superimposed to increasing absorptions related to nitrates. However it is still possible to follow the evolution of nitrites through the band at 1210 cm^{-1}. The maximum intensity of this band is reached after 5 min and maintained after 10 min (Fig. 4B, curve b and c). The intensity of such band is lower of that reached after 10 min in the absence of CO_2 (Fig. 4A, curve c). After 20 min (Fig. 4B, curve d) the intensity of nitrite band starts to decrease, as observed in the absence of CO_2. The presence of CO_2 in the feed decrease the total amount of stored NO_x down to 3×10^{-4} mol/g_{cat} (12% of the overall Ba loading).

When both CO_2 and H_2O are present (Fig. 4C), again the catalytic behavior closely resembles that previously described in the presence of CO_2 only at 250 °C, showing also in this case the formation of nitrites at the beginning of the storage, followed by their oxidation to nitrates. The formation of nitrites and nitrates is accompanied by the displacement of carbonates. The amount of NO_x stored in this case is very similar to that calculated in the presence of CO_2 only, i.e. near 2.6×10^{-4} mol/g_{cat} (11% of the overall Ba loading).

The results of the gas phase analysis performed on the flow micro-reactor are shown in Fig. 5. Under inert atmosphere, a dead time of about 95 s in the NO_x breakthrough is observed (curve a), while in the presence of CO_2 it decreases at about 17 s. The NO_2/NO ratio at the reactor outlet at steady-state (Table 1) is quite similar in the presence and in the absence of CO_2, thus pointing out the negligible role of CO_2 in the NO to NO_2 oxidation, whereas is decreased by the presence of water as already observed. In all cases, the stationary level reached by NO and NO_2 are far from chemical equilibrium of NO oxidation to NO_2, thus indicating that the reaction is kinetically controlled. Also at 250 °C the total amount

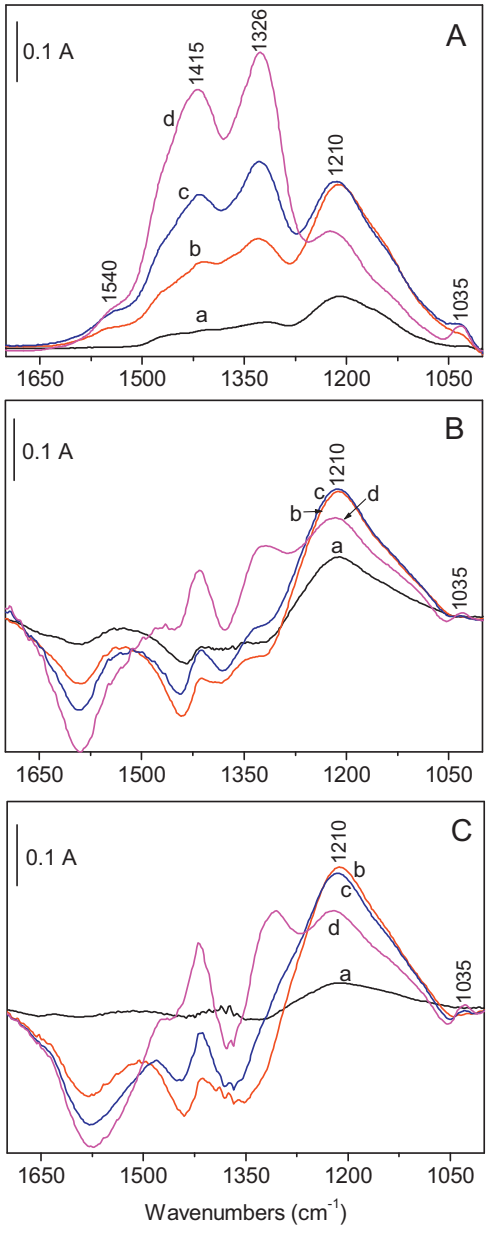

Fig. 4. Section A. FT-IR difference spectra of Pt-Ba/Al_2O_3 catalyst upon exposure to a stream of NO/O_2 (1000 ppm NO in Ar + O_2 3%, v/v) at 250 °C for increasing contact time. FT-IR spectra were recorded after 2 min (a), 5 min (b), 10 min (c) and 20 min (d). Subtrahend spectrum in section A: catalyst after activation cycles. Sections B is the corresponding measurements in the presence of CO_2 (1%, v/v) in the stream. Subtrahend spectrum in section B: catalyst upon exposure to the stream of CO_2 before NO/O_2 admission. Sections C is the corresponding measurements in the presence of CO_2 (1%, v/v) + H_2O (2%, v/v) in the stream. Subtrahend spectrum in section C: catalyst upon exposure to the stream of $CO_2 + H_2O$ before NO/O_2 admission.

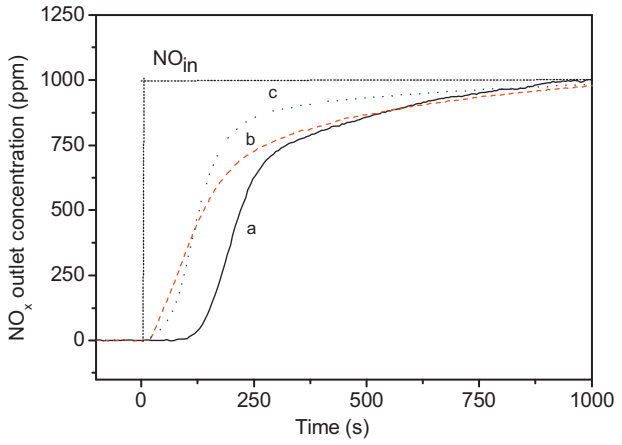

Fig. 5. NO_x outlet concentration during the storage phase at 250 °C over Pt-Ba/Al_2O_3 catalyst. 1000 ppm NO in He+ O_2 3% (v/v): curve a in He; curve b + CO_2 (1%, v/v) and curve c + CO_2 (1%, v/v) + H_2O (2%, v/v)

of desorbed CO_2 approaches the theoretical amount expected from the replacement of $BaCO_3$ with $Ba(NO_2)_2$ and $Ba(NO_3)_2$.

Finally, Fig. 6 shows the FT-IR spectra recorded as a function of time on stream during the NO_x storage at 350 °C in the absence (Fig. 6A) in the presence of CO_2 (Fig. 6B) and of $CO_2 + H_2O$ (Fig. 6 C). In the absence of CO_2 (Fig. 6A), IR spectra show that both nitrites (band at 1210 cm^{-1}) and nitrates (bands at 1415, 1320 and 1027 cm^{-1}) are almost simultaneously formed (Fig. 6A, curve a). After 10 min (Fig. 6A, curve c) the band at 1210 cm^{-1} related to nitrites is no more visible due to their oxidation into nitrates, while the nitrate bands continue to increase. In fact at this temperature the nitrate route is also active, as pointed out by the significant formation of NO_2 which is detected at the reactor outlet (Table 1). Near 4.3×10^{-4} mol/g_{cat} (18% of the overall Ba loading) of NO_x are stored at the end of the storage phase.

When NO_x adsorption is carried out in the presence of CO_2, again the analysis of the region 1700–1280 cm^{-1} in the FT-IR spectra (Fig. 6B) is complicated by the presence of negative bands related to the displacement of carbonates, superimposed to those of nitrates, as previously mentioned. Indeed, the bands at 1415 and 1312 cm^{-1} are related to ionic nitrates, but their intensity and in some extent also their position are invalidated by the negative bands related to carbonates. Notably, the band at 1210 cm^{-1} due to nitrites is hardly visible in this case, indicating that the amount of nitrites is much lower with respect to that observed without CO_2 at any time of contact. About 4.2×10^{-4} mol/g_{cat} (18% of the overall Ba loading) of NO_x are stored at the catalyst surface.

The presence of both CO_2 and H_2O does not change significantly the catalyst behavior and FT-IR spectra if compared to the presence of CO_2 only (compare Fig. 6B and C). Indeed, also in the presence of CO_2 and H_2O nitrites can be hardly identified. In these conditions 4.2×10^{-4} mol/g_{cat} (18% of the overall Ba loading) of NO_x are stored at the end of the storage phase.

The results of the gas phase analysis obtained with the powder plug-flow micro-reactor (Fig. 7) point out a significant dead time (120 s) in the NO_x breakthrough under inert atmosphere (trace a), while a significant decrease of the dead time is observed in the presence of CO_2 and CO_2/H_2O (15 s). In all cases, the concentrations of NO and NO_2 increase up to a steady state value. The NO_2/NO ratio (Table 1) is not significantly affected by the presence of CO_2 whereas it is decreased by the presence of water as already discussed.

As for the other investigated temperatures, also at 350 °C the total amounts of released CO_2 (not shown) well agree with those

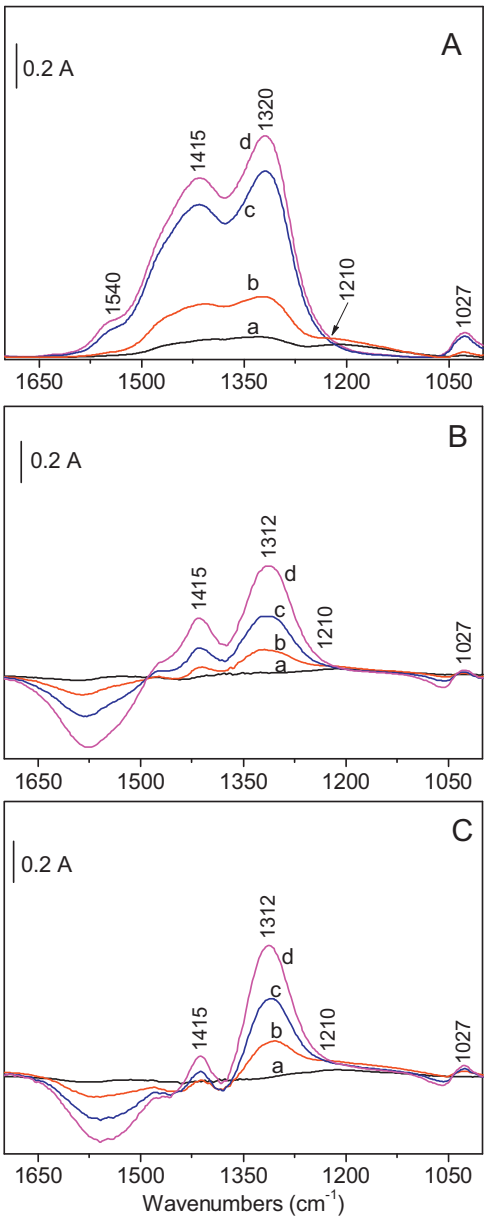

Fig. 6. Section A. FT-IR difference spectra of Pt-Ba/Al_2O_3 catalyst upon exposure to a stream of NO/O_2 (1000 ppm NO in Ar + O_2 3%, v/v) at 350 °C for increasing contact time. FT-IR spectra were recorded after 2 min (a), 5 min (b), 10 min (c) and 20 min (d). Subtrahend spectrum in section A: catalyst after activation cycles. Sections B is the corresponding measurements in the presence of CO_2 (1%, v/v) in the stream. Subtrahend spectrum in section B: catalyst upon exposure to the stream of CO_2 before NO/O_2 admission. Sections C is the corresponding measurements in the presence of CO_2 (1%, v/v) + H_2O (2%, v/v) in the stream. Subtrahend spectrum in section C: catalyst upon exposure to the stream of $CO_2 + H_2O$ before NO/O_2 admission.

expected from the stoichiometry of nitrate formation on Ba carbonates.

3.3. *Impact of CO_2 and water on the nitrite and nitrate routes for the NO_x storage*

It has been previously shown that the nitrite route, i.e. the adsorption of NO_x at a Pt-Ba couple leading to the formation of nitrite species, is the unique route active at low temperature (e.g. 150 °C) where selective formation of nitrites has been observed and where oxidation of NO to NO_2 is poor. At higher temperatures formation of nitrates has also been observed, as well as of NO_2 in the gas phase. Accordingly at these temperatures the nitrate pathway,

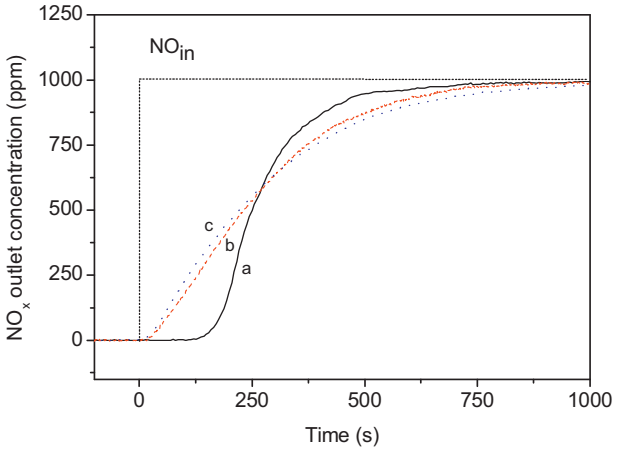

Fig. 7. NO_x outlet concentration during the storage phase at 350 °C over Pt-Ba/Al_2O_3 catalyst. 1000 ppm NO in He + O_2 3% (v/v): curve a in He; curve b + CO_2 (1%, v/v) and curve c + CO_2 (1%, v/v) + H_2O (2%, v/v)

involving the disproportion of NO_2 and leading to nitrate adspecies and NO, is also active in the storage of NO_x, although nitrates may also be formed by nitrite oxidation, formed in turn according to the so-called nitrite route.

CO_2 and NO_x compete for the same adsorption sites, being carbonates displaced during NO_x adsorption. As mentioned in Section 3.1, CO_2 adsorption allows to evaluate the overall fraction of surface sites available for carbonate formation, showing a maximum near 30% at 150 °C. Notably, the fraction of Ba sites involved in NO_x adsorption is always lower than that used for CO_2 adsorption and increases with temperature, at variance with what observed in the case of carbonate formation. At low temperature NO_x adsorption is limited by the slow rate of nitrite and nitrate formation, whereas at high temperature to the decrease of nitrate thermal stability.

The presence of CO_2 (and of CO_2 and water as well) has an impact on the formation of nitrites, as pointed out by the different intensity of the band at 1210 cm^{-1} ($\nu_{asym.}(NO_2)$ mode of nitrite species) in the presence and in the absence of CO_2 (and water). This is displayed in Fig. 8 (left side) which shows the amount of stored nitrites (evaluated from the linear intensity of the 1210 cm^{-1} band, i.e. the intensity of the band maximum, and using linear molar absorption coefficient reported in Ref. [11]) as a function of time in Ar (curves a), in Ar/CO_2 (curves b) and in Ar/CO_2/H_2O (curves c). Note that due to the overlap of bands of carbonates and of nitrates in the region 1300–1650 cm^{-1} the concentration of nitrates could not be followed directly.

In the absence of CO_2 the nitrite concentration shows the typical behavior of intermediate species [11]. In fact the nitrite concentration monotonically increase with time at low temperatures (150 °C), where almost only nitrites have been detected on the catalyst surface (if one neglect the small amounts of nitrates formed after prolonged contact), and show maxima at higher temperatures (250 °C and 350 °C), when nitrates are also observed. In particular at 350 °C nitrites are observed only at the very beginning of the storage, and after prolonged contact with NO only nitrates are present on the catalyst surface (see Fig. 4A).

Similar trends are apparent in the presence of CO_2, although differences are clearly visible in the nitrite concentration evolution with time. At 150 °C the influence of CO_2 on the nitrite concentration is negligible at the beginning of the exposure. After prolonged exposure the presence of CO_2 decreases the amount of nitrites stored at steady state, possibly due to the presence of residual carbonate species with high stability that nitrites are not able to displace. At 250 °C a small decrease of the maximum amount of stored nitrites is observed in the presence of CO_2; a much more pronounced effect is observed at 350 °C, although at this temperature the nitrite surface concentration is much lower even in the absence of CO_2. In fact at this temperature the maximum amount of nitrites measured in the presence of CO_2 is about 60% lower than that observed in the absence of CO_2.

It is of interest to compare the nitrite surface concentration estimated from FTIR data (Fig. 8, left side) with the total amounts of stored NO_x estimated from gas-phase analysis (Fig. 8, right side). At 150 °C the nitrite concentration and the total amounts of stored NO_x show similar behavior, in line with the observation that almost only nitrites are present at this temperature. The presence of CO_2 reduces the amounts of stored NO_x (i.e. 2.4×10^{-4} mol/g_{cat} vs. 3.7×10^{-4} mol/g_{cat}), in line with the decreased amount of stored nitrites (see Fig. 8, left panel). Water addition, along with CO_2, seems to have a slight beneficial effect in that it reduces the impact of CO_2.

At 250 °C the nitrite concentration exhibits a different behavior if compared to the total stored NO_x, being nitrates formed along with nitrites. Also in this case the stored NO_x are reduced in the presence of CO_2 (i.e. 3.0×10^{-4} mol/g_{cat} vs. 3.6×10^{-4} mol/g_{cat} at the end of exposure); the effect is even more evident in the presence of water as well. The observation that the total amounts of stored NO_x (i.e. nitrites + nitrates) is affected by the presence of CO_2 more than the nitrite concentration suggests that the nitrate formation is influenced by the presence of CO_2 as well. The presence of water further reduces the amounts of stored NO_x (but not of nitrites) possibly due to H_2O negative impact on the nitrate pathway (water inhibits the NO oxidation to NO_2).

Finally, at 350 °C nitrites represent only a minor fraction of the stored NO_x, being nitrates the dominant species; at such temperature the total amounts of NO_x stored at steady state are very similar at 350 °C in the presence of CO_2 and of H_2O and CO_2 as well. Considering that nitrite formation at this temperature is strongly inhibited by the presence of CO_2 (see Fig. 8, left side) whereas the amounts of stored NO_x are not apparently affected, it is concluded that the nitrate pathway is not affected by CO_2 (and water as well) at 350 °C, as already pointed out in a previous work of some of us [14].

The presence of CO_2 also impacts the dead time for NO_x breakthrough. Inspection of Figs. 3, 5 and 7 and of Table 1 clearly points out that in the absence of CO_2 the dead time for NO_x breakthrough is significant and increases with temperature, whereas in the presence of CO_2 (and of water as well) the dead time for NO_x breakthrough is not present or very short at any temperature. This picture is consistent with earlier proposal from some of us [14] where the dead time for NO_x breakthrough has been associated with the occurrence of the nitrite route and to the integral behavior of the reactor. In fact when the storage occurs via the nitrate route, i.e. according to the stoichiometry of the following disproportion reaction:

$$3NO_2 + BaCO_3 \rightarrow Ba(NO_3)_2 + NO \uparrow + CO_2 \quad (7)$$

the dead time for NO_x breakthrough is expected to be small being the NO_x storage accompanied by the evolution of NO. This is not the case of the "nitrite" pathway which implies the step-wise oxidation of NO to a surface nitrite over a Pt-Ba couple according to the stoichiometry of the overall reaction (6) [11]. In this light, the decrease of the dead time which is observed upon addition of CO_2 may be tentatively ascribed to the inhibiting effect of CO_2 on the nitrite pathway, mostly at high temperatures.

The inhibition effect of CO_2 on the nitrite route could be ascribed to the different thermal stability of the surface species involved in the storage, i.e. nitrites, nitrates and carbonates, and particularly to the ability of nitrites and nitrates to displace carbonates from surface sites.

In order to investigate the thermal stability of the involved surface species, nitrites, nitrates and carbonates have been

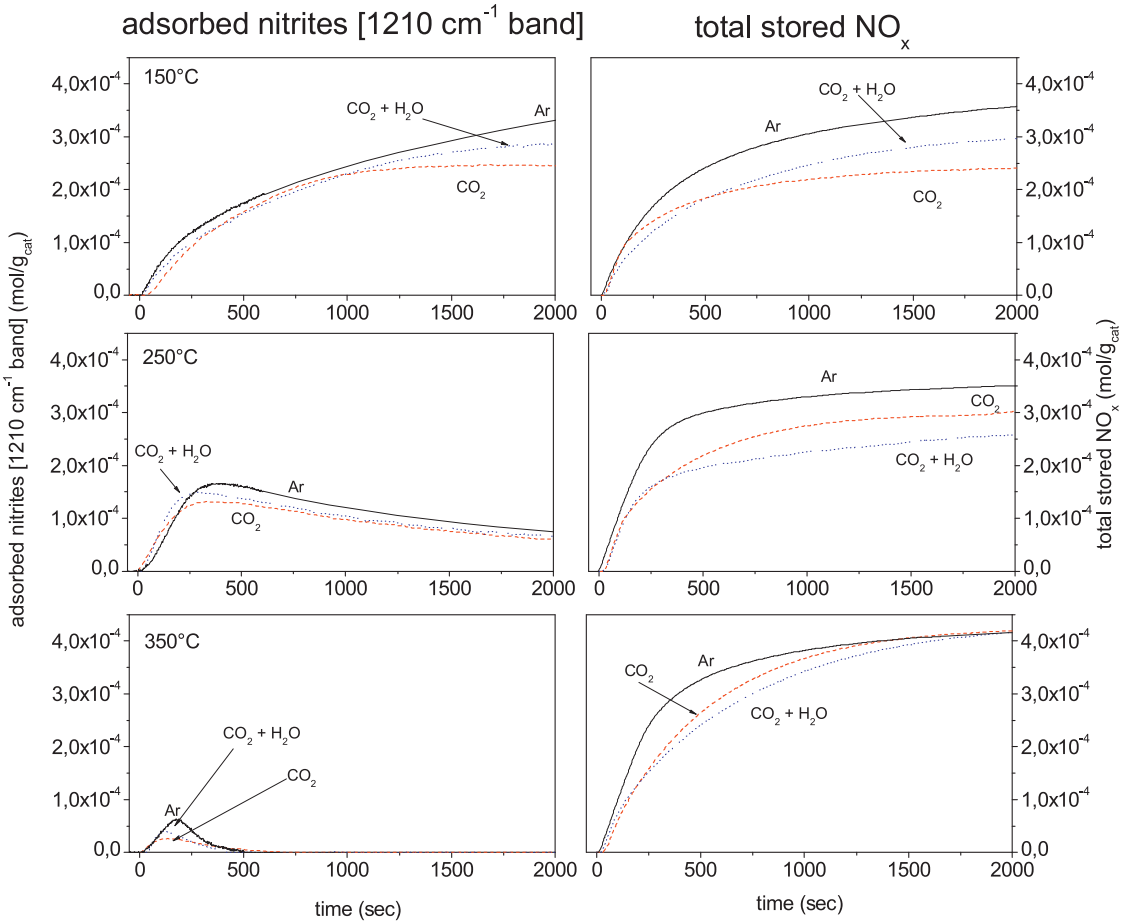

Fig. 8. Amount of stored nitrites (evaluated by the linear intensity of the band at 1210 cm^{-1})and of the total amount of stored NO_x as a function of time during the NO_x storage at 150 °C (A), 250 °C (B) and 350 °C (C) in Ar (a), in the presence of CO_2 (1%, v/v) (b) and in the presence of CO_2 (1%, v/v) + H_2O (2%, v/v) (c) in the stream.

individually adsorbed at 100 °C, and evacuated at increasing temperature in the range 100–400 °C (see experimental). Fig. 9 shows the integrated intensities of IR absorptions of nitrites (Fig. 9A), nitrates (Fig. 9B) and carbonates (Fig. 9C) in the range 1700–1100 cm^{-1} as a function of the evacuation temperature. The integrated intensity of the bands in the presence of the gas phase at 100 °C has been set at 100%. In order to compare thermal stabilities of nitrites, nitrates and carbonates the slopes of the curves in Fig. 9 are compared: the greater the slope, the lower the thermal stability is in the considered temperature range. However, it is important to underline that nitrates and carbonates are present on the catalyst with different geometries (bidentate and ionic) that reasonably show different absorption coefficients; this is not the case for nitrites that show only one geometry. Different absorption coefficients of the different species may invalidate this kind of evaluation if during the desorption process the relative population of the different species changes. However during the desorption process at increasing temperature the relative population of different species do not change in a relevant way (spectra not reported for sake of brevity), and this allows a safe comparison of the thermal stability of the different surface species.

As apparent from Fig. 9B, nitrates are very stable up to 350 °C: accordingly these species, when formed, are able to displace the less stable carbonate species, being decomposed starting from 100 °C (see Fig. 9C). A different picture is apparent in the case of nitrites (Fig. 9A). At low temperature nitrites show comparable stability with respect to carbonates, so nitrites are almost quantitatively formed at the expenses of carbonates. However, at high contact time the displacement of the most stable carbonate species is more difficult, resulting in a lower total amount of stored NO_x at steady state. On the other hand, at high temperature the nitrite stability is lower than that of carbonates, so nitrites are not able to displace these species. In fact the formation of nitrites results strongly inhibited by CO_2 that lowers of about 60% the maximum amount of nitrites with respect to the case in the absence of CO_2 at 350 °C (Fig. 8).

In summary, the ability of nitrites to displace carbonates from the catalyst surface decreases with increasing temperature, while nitrates are able to displace carbonates at high temperature as well being more stable.

Concerning the role of water, Szanyi et al. [24] demonstrated that in the presence of water surface Ba-nitrates convert to bulk Ba-nitrates. Nevertheless, they showed that the amount of NO_x taken up at 300 K by the storage material is essentially unaffected by the presence of water. Some of us in a recent paper [25] showed that surface hydroxylation is responsible for the conversion of bidentate nitrates into ionic ones. In the present paper, concerning the role of water (along with CO_2) on the nitrite formation, inspection of Fig. 8 points out that at low temperature water slightly increases the total amount of stored NO_x with respect to the presence of CO_2 only. This is reasonably due to the transformation of bidentate carbonates into ionic ones operated by water, as mentioned in Section 3.1. It is expected that ionic carbonates show different thermal stability with respect to bidentate ones, modifying the total amount of stored NO_x at steady state. At 250 °C the amount of nitrites is not sensibly modified by water (Fig. 8, left side), but the total amount of stored NO_x (Fig. 8, right side) is significantly lower with respect Ar and CO_2 only, since water inhibits the oxidation of NO to NO_2 and,

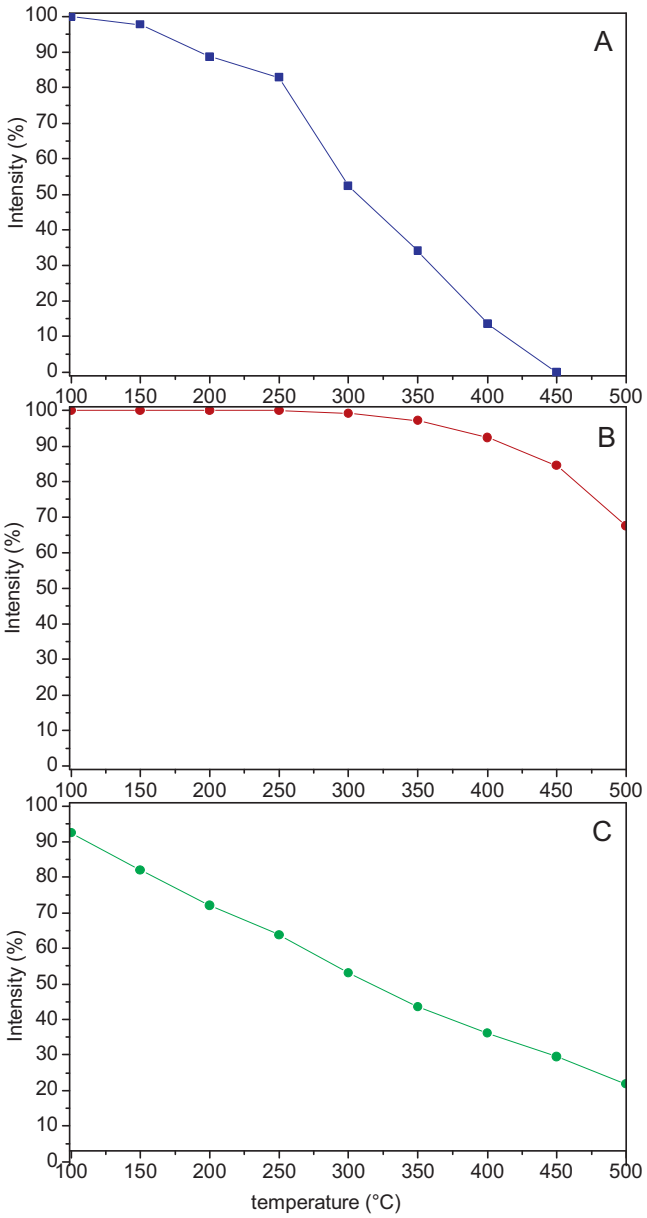

Fig. 9. Thermal stability of species formed on Pt-Ba/Al_2O_3 catalyst upon adsorption of (A) NO/O_2 (1:10) mixture (nitrites); (B) NO_2 (nitrates); and (C) CO_2 (carbonates) at 100 °C, evaluated by the integrated intensities of the IR absorptions in the range 1700–1100 cm^{-1} range vs. the evacuation temperature. The integrated intensities of the bands at 100 °C in the presence of the gas phase is set to 100%.

as a consequence, inhibits the nitrate route. The inhibitor effect of water onto NO oxidation decreases on increasing temperature due to the higher rate of NO oxidation. Accordingly at 350 °C the water effect on the total amount of stored NO_x is negligible.

4. Conclusions

The data herein presented converge in indicating that over Pt-Ba/Al_2O_3 LNT catalyst the storage of NO_x in the presence of oxygen and CO_2 under dry and wet conditions occurs through two pathways operating simultaneously, as in the absence of CO_2 and H_2O, i.e. the nitrite and the nitrate pathways. The nitrite route is the unique pathway operating at low temperature (i.e. 150 °C) and involves the formation of surface nitrites only; the nitrate route, operating at higher temperature (i.e. ≥200 °C) along with the nitrite pathway, involves NO oxidation to NO_2 over Pt and its subsequent adsorption on Ba phase in the form of nitrates. Nitrates may also form upon nitrite oxidation.

The combined use of *operando* FT-IR spectroscopy and the transient response method has provided additional information which allowed to highlight the influence of CO_2 and H_2O on the NO_x storage. In particular, the presence of CO_2 does not significantly affect the NO_x storage at low temperature (150 °C) where formation of nitrites only has been observed. This indicates that at low temperatures the nitrite route for NO_x storage is not affected by the presence of CO_2. On the other hand, the nitrite route is progressively inhibited by CO_2 upon increasing the temperature, and this result in a decrease of the dead time for the NO_x breakthrough that has been associated to the occurrence of the nitrite route. However, since the presence of CO_2 does not affect the NO oxidation to NO_2 and the occurrence of the nitrate route with nitrates well able to displace carbonates, the amounts of stored NO_x are only slightly decreased by CO_2 at 350 °C where NO oxidation to NO_2 is fast. On the other hand, on the base of gas phase analysis at 250 °C and 150 °C the presence of CO_2 decreases the amounts of stored NO_x. The change with temperature of the inhibition of CO_2 on the nitrite route can be related to the different thermal stability of nitrites and carbonates on varying temperature, with nitrite ability to displace carbonates that decreases on increasing temperature.

The results obtained during the NO_x storage in the presence of CO_2 in wet conditions are very similar to those obtained in dry conditions at all the temperatures studied, pointing out only minor effect of water on the NO_x storage.

References

[1] W.S. Epling, L.E. Campbell, A. Yezerets, N.W. Currier, J.E. Parks, Catal. Rev. Sci. Eng. 46 (2004) 163.
[2] S.I. Matsumoto, Catal. Today 90 (2004) 183.
[3] M. Piacentini, M. Maciejewski, A. Baiker, Appl. Catal. B: Environ. 60 (2005) 265.
[4] T. Szailer, J.H. Kwak, D.H. Kim, J.C. Hanson, C.H.F. Peden, J. Szanyi, J. Catal. 239 (2006) 51.
[5] T.J. Toops, D.B. Smith, W.P. Partridge, Catal. Today 114 (2006) 112.
[6] S.M. Park, J.W. Park, H.P. Ha, H.S. Han, G. Seo, J. Mol, Catal. A: Chem. 273 (2007) 64.
[7] M. Al-Harbi, D. Radtke, W.S. Epling, Appl. Catal. B: Environ. 96 (2010) 524.
[8] T. Lesage, J. Saussey, S. Malo, M. Hervieu, C. Hedouin, G. Blanchard, M. Daturi, Appl. Catal. B-Environ. 72 (2007) 166.
[9] F. Prinetto, G. Ghiotti, I. Nova, L. Castoldi, L. Lietti, E. Tronconi, P. Forzatti, Phys. Chem. Chem. Phys. 5 (2003) 4428.
[10] I. Nova, L. Castoldi, L. Lietti, E. Tronconi, P. Forzatti, F. Prinetto, G. Ghiotti, J. Catal. 222 (2004) 377.
[11] L. Lietti, M. Daturi, V. Blasin-Aube, G. Ghiotti, F. Prinetto, P. Forzatti, ChemCatChem 4 (2012) 55.
[12] S.S. Chaugule, V.F. Kispersky, J.L. Ratts, A. Yezerets, N.W. Currier, F.H. Ribeiro, W.N. Delgass, Appl. Catal. B: Environ. 107 (2011) 26.
[13] B.M. Weiss, K.B. Caldwell, E. Iglesia, J. Phys. Chem. C 115 (2011) 6561.
[14] F. Frola, F. Prinetto, G. Ghiotti, L. Castoldi, I. Nova, L. Lietti, P. Forzatti, Catal. Today 126 (2007) 81.
[15] F. Prinetto, G. Ghiotti, I. Nova, L. Lietti, E. Tronconi, P. Forzatti, J. Phys. Chem. C 105 (2001) 12732.
[16] F. Frola, M. Manzoli, F. Prinetto, G. Ghiotti, L. Castoldi, L. Lietti, J. Phys. Chem. C 112 (2008) 12869.
[17] J.C. Lavalley, Catal. Today 27 (1996) 377.
[18] S. Morandi, F. Prinetto, G. Ghiotti, L. Castoldi, L. Lietti, P. Forzatti, Unpublished results.
[19] C. Morterra, G. Magnacca, Catal. Today 27 (1996) 497.
[20] W.S. Epling, C.H.F. Peden, J. Szanyi, J. Phys. Chem. C 112 (2008) 10952.
[21] L. Olsson, M. Abul-Milh, H. Karlsson, E. Jobson, P. Thormahlen, A. Hinz, Top. Catal. 30–1 (2004) 85.
[22] S.S. Mulla, N. Chen, L. Cumaranatunge, W.N. Delgass, W.S. Epling, F.H. Ribeiro, Catal. Today 114 (2006) 57.
[23] C.M.L. Scholz, V.R. Gangwal, M.H.J.M. de Croon, J.C. Schouten, Appl. Catal. B: Environ. 71 (2007) 143.
[24] J. Szanyi, J.H. Kwak, D.H. Kim, X. Wang, R. Chimentao, J. Hanson, W.S. Epling, C.H.F. Peden, J. Phys. Chem. C 111 (2007) 4678.
[25] S. Morandi, F. Prinetto, L. Castoldi, L. Lietti, P. Forzatti, G. Ghiotti, Phys. Chem. Chem. Phys. 15 (2013) 13409.